ANNUAL COOLING PERFORMANC PREDICTION OF AN ADSORPTION CHILLER APPLIED SYSTEM BASED ON A NUMERICAL MODEL

Fang He[1], Hong Z. Liu[1], Katsunori Nagano[1] and Junya Togawa[2]

[1] Hokkaido University, Sapporo (Japan)

[2] Nihon Netsugen System, Tokyo (Japan)

Abstract

This study focuses on the annual cooling performance prediction of the Adsorption Chiller (AC). A three-dimensional numerical calculation program was built in our previous study for the parameter analysis of the AC, and the results were applied to develop an approximate function of COP and SCP, thus the performance calculation period of the AC can be reduced obviously and the annual prediction based on the continuous temperature condition was available. Then this approximate function was employed to describe the performance of the AC, which provide cooling capacity for a system numerical model. The real cooling load data of a building and the climate data from March 2022 to February 2023 were applied. This model was proved to work well for the annual cooling performance prediction. Moreover, the performance of this AC was evaluated for its practical application.

Keywords: Adsorption Chiller (AC), Annual cooling performance prediction, Numerical model

1. Introduction

With the development of the global economic, the thermal comfort requirement has increased in the development countries (Pan Q.W. and Wang R.Z., 2018). The traditional compression-type air conditioners market booming is expected, however, problems such as CO_2 emissions and ozone layer depletion need to be addressed (Lu Z.S. and Wang R.Z., 2013). The adsorption chiller (AC), which is one of the thermally driven heat pumps, is considered an attractive solution. An AC can provide cooling capacity by the low-grade heat sources from 60 to 80 ◦C (Sapienza A. et al., 2011), e.g., factory exhaust or hot water from a solar water heater (Akahira A. et al., 2004)(Pan Q.W. and Wang R.Z., 2017) (Sapienza A. et al., 2011). AC is an environmentally friendly technology for its natural refrigerants such as water and ammonia. However, some disadvantages of AC hamper its popularization. The coefficient of performance (COP) is near 0.5 (J. Romero R. et al., 2001)(Jung-Yang San and Tsai Fu-Kang, 2014), which is lower than other types of thermally driven ACs (J. Romero R. et al., 2001)(Manu S. and Chandrashekar T.K., 2016)(Srikhirin P. et al., 2001). The initial cost of the AC is expensive due to its exorbitant adsorbent material (He F. et al., 2022). In addition, the more compact entire AC body is necessary. These disadvantages result in popularization barrier of AC.

In order to overcome these disadvantages mentioned above, a kind of composite material, which called Wakkanai Siliceous Shale (WSS) impregnated with 20 wt. % of LiCl, was proposed by our team (Nakabayashi S. et al., 2011). Several experiments applied this composite material as adsorbent have been conducted to investigate the cooling performance of composite material AC (He F. et al., 2022) (Liu H. et al., 2011)(Togawa J. et al., 2020). It was proved to be a competitive adsorbent material compared with other adsorbent due to its relatively high performance and acceptable price (He F. et al., 2020)(Togawa J. et al., 2020). Then the numerical model has been built for the performance prediction of the AC (He F. et al., 2023)(Seol S.H. et al., 2020). On the other hand, the annual performance prediction of AC system by the numerical model is unavailable due to its large amount of calculation time. The performance prediction speed at each condition need improvement.

In this study, author propose approximate functions to achieve the fast calculation of AC cooling performance.

10.18086/swc.2023.04.04 Available at http://proceedings.ises.org

The numerical model built in our previous study is applied to calculate several representative COP and Specific Cooling Power (SCP)(He F. et al., 2023). The approximately functions are fitted based on the representative of COP and SCP and proved to be creditable. Then a model of AC system, in which the AC is employed to provide cooling capacity, is established for the annual cooling performance prediction. A municipal government office building of Japan is chosen as the target building. The annual cooling load of this building in period from March 2022 to February 2023 is picked up and introduced to this AC system. The area of the solar collector, hot water volume coefficient and the adsorbent weight are evaluated for the optimization as the parameters, and the cover rate and payback year are introduced as the evaluation indices. The results indicate the possibility of using AC to provide cooling capacity, and the minimum payback years in different cover rates are calculated.

2. Methodology

2.1. AC system

In this study, a numerical model was built for the annual cooling performance prediction, as shown in **Fig.1**. The AC system consists of the AC, the solar collector with the hot water tank, and the cooling tower. The target building annual cooling load of a prediction period is introduced to the AC system to determine the cooling capacity. The annual climate data of the same period is download from the weather bureau home page. Based on the annual radiation data, temperature of the hot water boiled by the solar collector can be calculated. The produced hot water is stored in the hot water tank and applied as the regeneration hot water of the AC. Meanwhile the temperature of the cooling water produced by the cooling water is calculated based on the annual temperature and humidity. The cooling water is flowed into the AC for the sorption and condensation process. According to the temperature of the hot water, cooling water and the cooling load, cycle period of the AC is controlled to increase COP while the enough cooling capacity is provided. In addition, the compress type air-conditioner is employed to provide extra cooling capacity while AC can't cover all the cooling load.

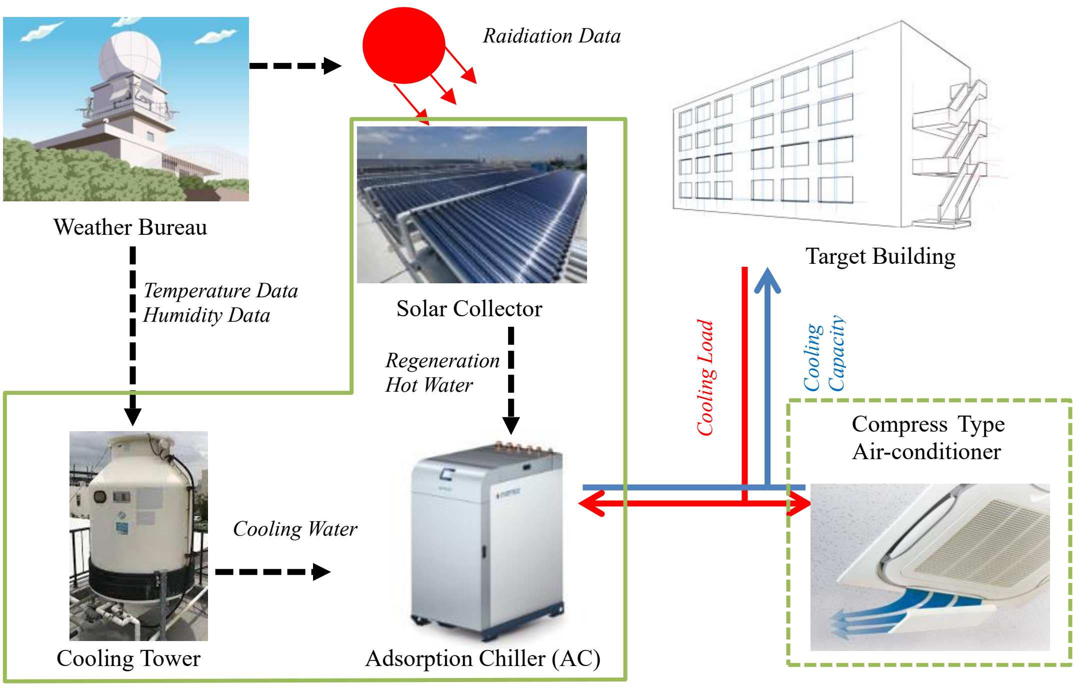

Fig. 1: Schematic of the AC system

2.2. Target building and prediction period

Target building is a municipal government office building, which is in Kamizaki City, Fukuoka province, Japan. The prediction period is from March 2022 to February 2023. The cooling load is recorded every minute, it is exchanged and expressed every hour, as shown in **Fig.2**.

The location of the target building is on south of Japan, which is humid subtropical climate. The cooling load

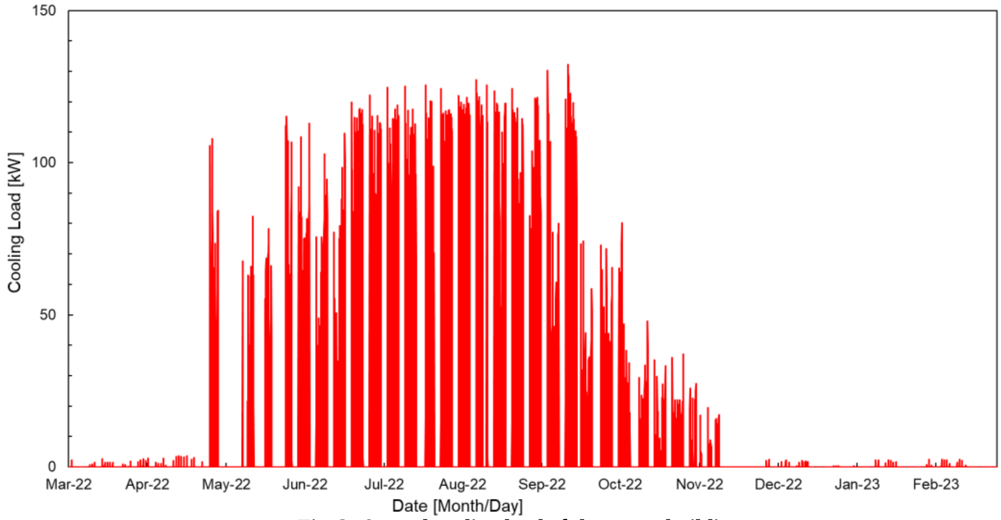

Fig. 2: Annual cooling load of the target building

can be clearly observed from end of April to middle of October. The highest cooling load approach 130 kW, however, the cooling load is generally up to 120 kW. It influences the designing of the AC capacity.

2.3. Numerical model

2.3.1. Performance functions of AC

Then approximate functions of AC performance are established. The 3-dimensional numerical model built in our previous study is employed to determine the representative COP and SCP (He F. et al., 2023). The calculation conditions are shown in **Tab.1**. In this study, AC is only used for the space cooling, hence the evaporation temperature is set at constant 15 ℃ instead of the dehumidification temperature 7 ℃.

Tab. 1: Calculation conditions for the representative COP and SCP

	Regeneration Temperature [℃]	Sorption/Condensation Temperature [℃]	Evaporation Temperature [℃]	Cycle Period [min]
Range	55-80	25-40	15	2-30
Interval	5	5	Constant	2

$$Q_{\mathrm{c}} = (\boldsymbol{a}_1 \times T_{\mathrm{reg}} + \boldsymbol{a}_2 \times T_{\mathrm{sor}}{}^{\boldsymbol{a}_3}) \times \arctan\,(\boldsymbol{a}_4 \times t_{\mathrm{cyc}}) \quad \text{(eq. 1)}$$

$$Q_{\mathrm{reg}} = (\boldsymbol{b}_1 \times T_{\mathrm{reg}} + \boldsymbol{b}_2 \times T_{\mathrm{sor}}{}^{\boldsymbol{b}_3}) \times \arctan\left(\boldsymbol{b}_4 \times t_{\mathrm{cyc}}\right) + \boldsymbol{b}_5(T_{\mathrm{reg}} - T_{\mathrm{sor}}) \times H_{\mathrm{sensible}} \quad \text{(eq. 2)}$$

Tab. 2: Parameters of the approximate functions

	1	2	3	4	5
a	4.831×10	-7.080	1.640	2.360×10^{-2}	-
b	7.492×10	-1.674×10	1.524	2.184×10^{-2}	4.367×10^{-1}

Based on the calculation results, the approximate functions are fitted, as shown in **eq.(1)** and **(2)**. The parameters of the approximate functions are listed in **Tab.2**. Then the accumulated cooling/regeneration amounts of the calculation results and the approximate functions prediction are shown in **Fig.3**. The line is the approximate functions and the cycle mark is the calculation results. The approximate functions fit the

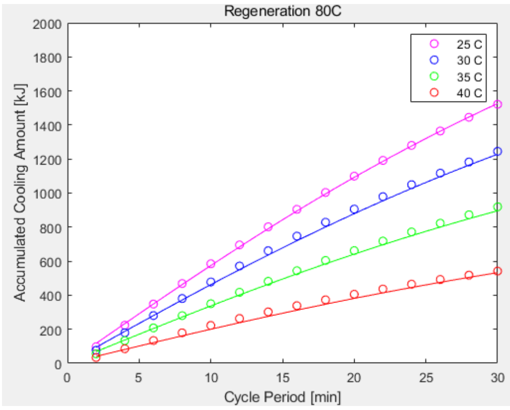

(a): Accumualted cooling amount at regeneration temperature of 80℃

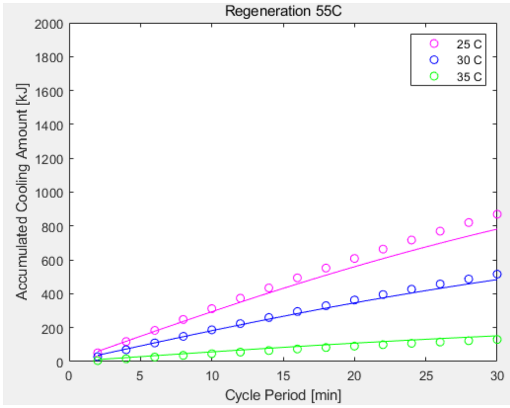

(b): Accumualted cooling amount at regeneration temperature of 55℃

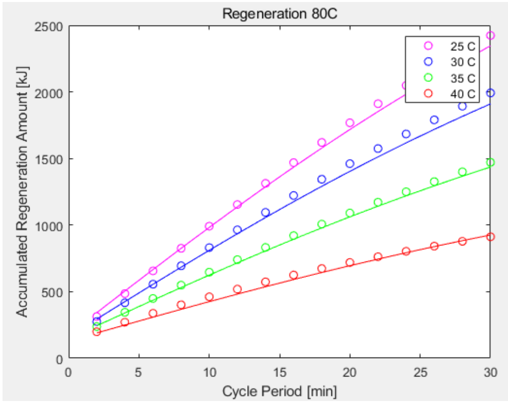

(c): Accumualted regeneration amount at regeneration temperature of 80℃

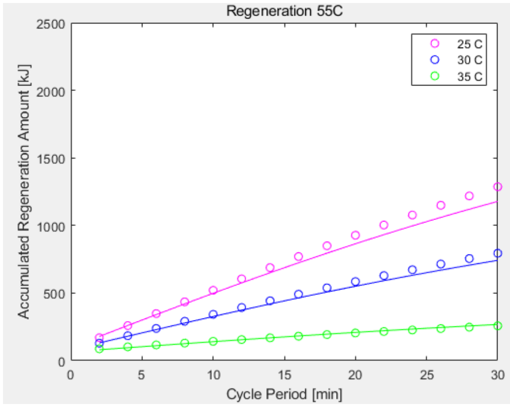

(d): Accumualted regeneration amount at regeneration temperature of 55℃

Fig. 3: Comparison of the calculated results and the approximate functions prediction

calculation results well at regeneration temperature of 80 ℃ for both of the accumulated cooling/regeneration amount. For the cases that the regeneration temperature is 55 ℃, the error between the approximate functions and the calculated results occurred while the cooling temperature decrease to 25 ℃. In this study, the AC system is mainly used in summer, thus this part of error is considered to be acceptable and this approximate function fit the calculation results very well in all the field.

2.3.2. Annual climate data

The annual climate data during March 2022 to February 2023 is down from the home page of the weather bureau. The annual dry bulb temperature and the annual solar radiation are shown in **Fig.4.(a)** and **Fig.4.(b)**, respectively.

2.3.3. Solar collector and cooling tower

The solar collector is applied to produce the hot water. The hot water temperature can be expressed by **eq.(3)**. According to the solar radiation data of **Fig.4.(b)** in section 2.3.2, the hot water can be heated in the solar collector, as the first part on the right side of the equation shows. Meanwhile, the heat loss between the boiled water and the ambient environment is expressed by the second part on the right side of the equation. The boiled water is stored in the hot water tank, the heat loss between the hot water tank and the ambient environment is determined as the third part on the right side of the equation. In addition, the fourth part is the regeneration capacity. In addition, the hot water temperature is limited to lower than 90 ℃ to avoid boiling.

$$c_{\mathrm{w}}\frac{dT_{\mathrm{w}}}{dt} = \eta A_{\mathrm{SC}}E - F_{\mathrm{L}}A_{\mathrm{SC}}\left(T_{\mathrm{w}} - T_{\mathrm{drybulb}}\right) - 6.48\left(T_{\mathrm{w}} - T_{\mathrm{drybulb}}\right)V_{\mathrm{w}} - \dot{Q}_{\mathrm{reg}} \qquad \text{(eq. 3)}$$

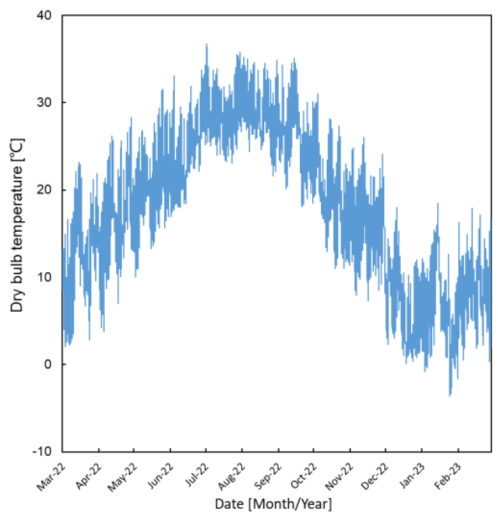

(a): Annual dry bulb temperature

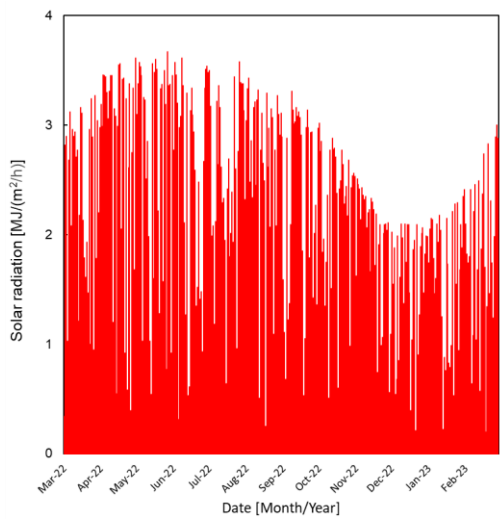

(b): Annual solar radiation

Fig. 4: Annual climate data

$$en_{\mathrm{drybulb}} = 1.006 \times T_{\mathrm{drybulb}} + (1.805 \times T_{\mathrm{drybulb}} + 2501) \times RH \quad \text{(eq. 4)}$$

$$en_{\mathrm{wetbulb}} = 1.006 \times T_{\mathrm{wetbulb}} + (1.805 \times T_{\mathrm{wetbulb}} + 2501) \times RH \quad \text{(eq. 5)}$$

$$C = en_{\mathrm{drybulb}} - en_{\mathrm{wetbulb}} - (\frac{T_{\mathrm{drybulb}}}{1000} - RH) \times 4.2 \times T_{\mathrm{wetbulb}} \quad \text{(eq. 6)}$$

$$T_{\mathrm{ct-out}} = T_{\mathrm{sor-out}} - (0.648 \times T_{\mathrm{sor-out}} - 0.439 \times T_{\mathrm{wetbulb}} + 0.316 \times C - 10.142) - (0.648 \times T_{\mathrm{sor-out}} - 0.439 \times T_{\mathrm{wetbulb}} + 0.316 \times C - 10.142) \times 0.39 \times \rho_{\mathrm{w}} \times \dot{m} \quad \text{(eq. 7)}$$

Based on the annual climate data of the dry bulb temperature, the wet bulb temperature and the relative humidity, the temperature from the cooling tower is calculated by **eq.(4)-(7)**.

2.4. Evaluation indices

In this study, coefficient of performance (COP) and specific cooling power (SCP) are applied to investigate the cooling performance of the AC. Based on the approximate function predictions of **eq.(1)** and **eq.(2)**, COP and SCP can be expressed by **eq.(8)**. and **eq.(9)**.

$$\mathrm{COP} = \frac{Q_{\mathrm{c}}}{Q_{\mathrm{reg}}} \quad \text{(eq. 8)}$$

$$\mathrm{SCP} = \frac{Q_{\mathrm{c}}}{m_{\mathrm{adsorbent}} t_{\mathrm{cyc}}} \quad \text{(eq. 9)}$$

In this study, the cover rate (*CR*) and the payback year are introduced to evaluate the practicality of this AC system. The cover rate is calculated by **eq.(10)**, which is the ratio of the annual average cooling capacity provided by AC system versus the annual average cooling load of target building. High cover rate indicates sufficient cooling capacity.

$$CR = \frac{Q_{\mathrm{annual\ average\ cooling\ capacity}}}{Q_{\mathrm{annual\ average\ cooling\ load}}} \quad \text{(eq. 10)}$$

Payback year (PY) is determined by **eq.(11)**. $Cost_{ac,in}$ is the initial cost of the AC and $Cost_{com,in}$ is the initial cost of the compress type air-conditioner, their calculation equations are **eq.(13)** and **eq.(14)**, respectively. The electricity reduction is calculated by **eq.(15)**. Thus, the initial cost and running cost of the AC system are compared with those of the compress type air-conditioner to calculate the payback year. In addition, the introduction grant from the government can be expected due to the renewable energy application. The payback year with the 2/3 of grant is expressed by **eq.(12)**. All the coefficients noticed in **eqs.(11)-(15)** are listed in **Tab.3**.

$$PY = \frac{Cost_{\mathrm{ac,ini}} - Cost_{\mathrm{com,ini}}}{Electricity\ Reduction \times (Price_{\mathrm{ele}} + Emission_{\mathrm{co2}} \times Price_{\mathrm{co2}})} \tag{eq. 11}$$

$$PY_{\mathrm{Grant}} = \frac{Cost_{\mathrm{ac,ini}} + Cost_{\mathrm{SC}} + Cost_{\mathrm{HT}} \times (1 - \frac{2}{3}) - Cost_{\mathrm{com,ini}}}{Electricity\ Reduction \times (Price_{\mathrm{ele}} + Emission_{\mathrm{co2}} \times Price_{\mathrm{co2}})} \tag{eq. 12}$$

$$Cost_{\mathrm{ac,in}} = m_{\mathrm{adsorbent}} \times \mathrm{SCP_{max}} \times Coe_{\mathrm{AC}} + A_{\mathrm{SC}} \times Coe_{\mathrm{SC}} + A_{\mathrm{SC}} \times Coe_{\mathrm{Vol}} \times Coe_{\mathrm{HT}} \tag{eq. 13}$$

$$Cost_{\mathrm{com,in}} = m_{\mathrm{adsorbent}} \times \mathrm{SCP_{max}} \times Coe_{\mathrm{com}} \tag{eq. 14}$$

$$Electricity\ Reduction = \frac{Accumulated\ annual\ cooling\ capacity}{\mathrm{COP_{com}}} \tag{eq. 15}$$

Tab. 3: Coefficients of indice

Coe_{AC} [JPY/kW]	Coe_{SC} [JPY/m^2]	Coe_{HT} [JPY/L]	Coe_{com} [JPY/kW]	$Price_{ele}$ [JPY/kWh]	$Price_{co2}$ [JPY/kg]	$Emission_{co2}$ [kg/kWh]	COP_{com} [-]
182500	15000	400	50000	43.14	8.263	0.299	3.5

3. Results and discussion

3.1. Annual performance prediction

The cooling performance and the payback year of the AC system compared with the compress type air-conditioners are influenced by the adsorbent weight, the solar collector area and the hot water tank volume coefficient. Firstly, they are fixed as shown in **Tab.4.**

Tab. 4: Coefficients of indice

Parameter	$m_{adsorbent}$ [kg]	Coe_{Vol} [L/m^2]	A_{SC} [m^2]
Volume	240	100	1200

The results of annual performance prediction are shown in **Fig.5**. The annual cooling load/capacity are shown in **Fig.5.(a)**. Most of the cooling load can be covered by the cooling capacity in May, October and November. However, the cooling capacity provided by the AC system is obviously insufficient during the summer. The annual regeneration and sorption temperature are shown in **Fig.5.(b)**. The annual cooling temperature transient is as regular as the annual dry bulb temperature transient is shown in **Fig.4.(a)**. The regeneration temperature is down to 50 ℃ for several times at the same period the cooling capacity can't cover the cooling load. It indicates the insufficiency of the solar collector area and the hot water tank volume. The accumulated cooling load and capacity per month are summarized in **Fig.5.(c)**. Obviously, the monthly cooling capacities can't cover the cooling load from June to September. Annual COP and SCP transients are shown in **Fig.5.(d)**. Annual COP is kept around 0.65 generally and decreased to 0.4 sometimes, meanwhile annual SCP is changed from 0.05 kW/kg – 0.45 kW/kg. In this case, the CR of this case is 85.89 % based on the data of **Fig.5.(c)**. The payback year PY and PY_{grant} are 104.7 years and 34.9 years, respectively. Annual electricity consumption amount of 17420.2 kWh, which equivalent 7.58 ton of CO_2 emissions. The AC system is proved to be effective

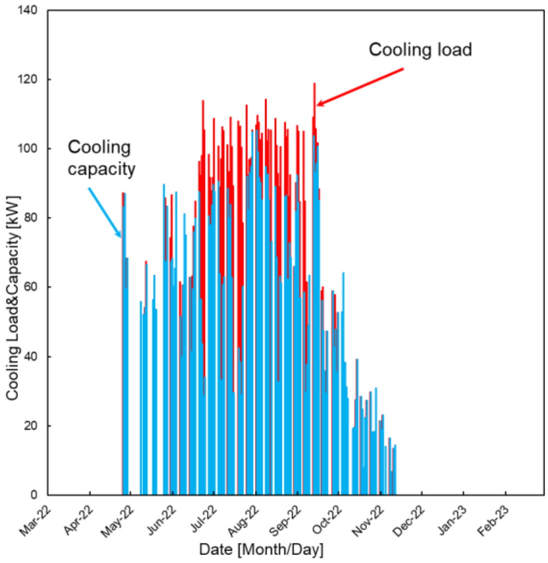

(a): Annual cooling load/capacity

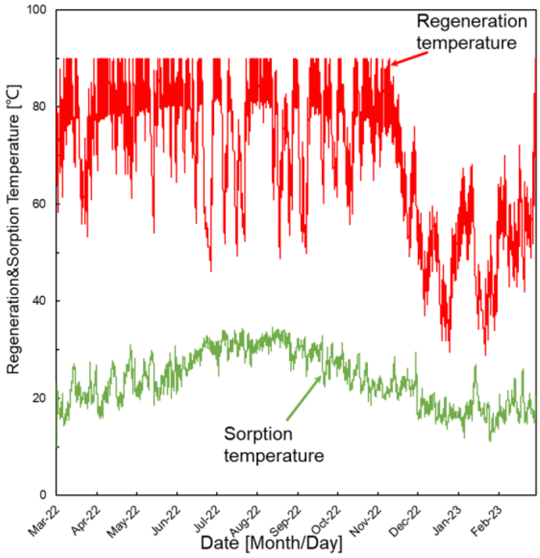

(b): Annual regeneration/sorption temperature

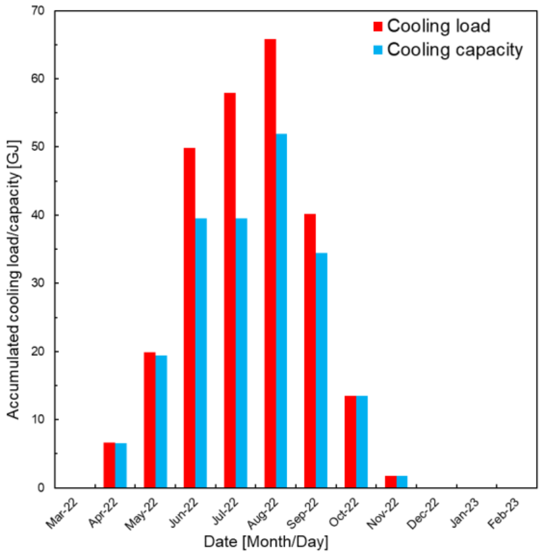

(b): Accumulated cooling load/capacity

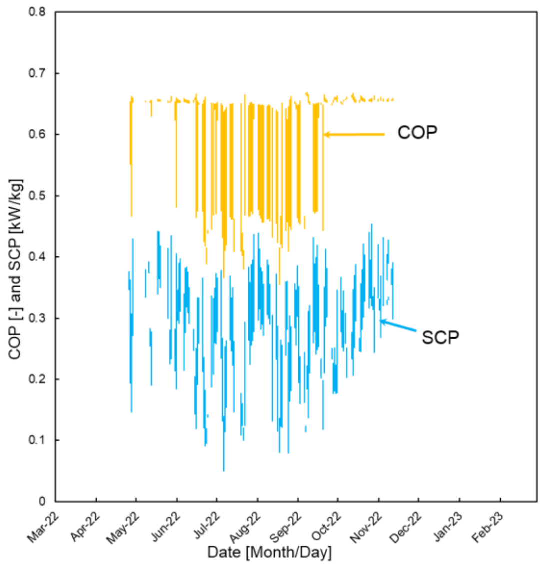

(d): Annual COP and SCP

Fig. 5: Annual climate data

to reduce the electricity consumption and CO_2 emissions.

This entire annual cooling performance prediction need about 40 second to calculate. It is much faster compared with the previous 3-dimentional model, which takes more than 1 hour for a set of temperature and cycle period conditions.

3.2. Parameter study

3.2.1. Adsorbent

The adsorbent weight of the AC is studied to evaluate the cooling performance of the AC system. Coe_{Vol} and A_{SC} are fix as shown in **Tab.4**, meanwhile $m_{\mathrm{adsorbent}}$ is changed from 20 kg to 480 kg at interval of 20 kg.

The prediction results are shown in **Fig.6(a)**. With the increase of the adsorbent weight, the cover rate shows a quick increasing up to 98.34 %. The more adsorbent applied in the AC, the bigger capacity can be provided by the AC to cover the cooling load. The PY is reduced to 100.0 years while the adsorbent weight increases to 280 kg, meanwhile the PY_{grant} is reduced to 33.3 years. Then the PY is stable around 100 years and the PY_{grant} is stable around 35 years. **Fig.6(a)** express the annual average COP and SCP. COP increase and became stable while the $m_{\mathrm{adsorbent}}$ increase up to 260 kg, meanwhile SCP decrease to less than 0.3 kW/kg. Obviously, too little

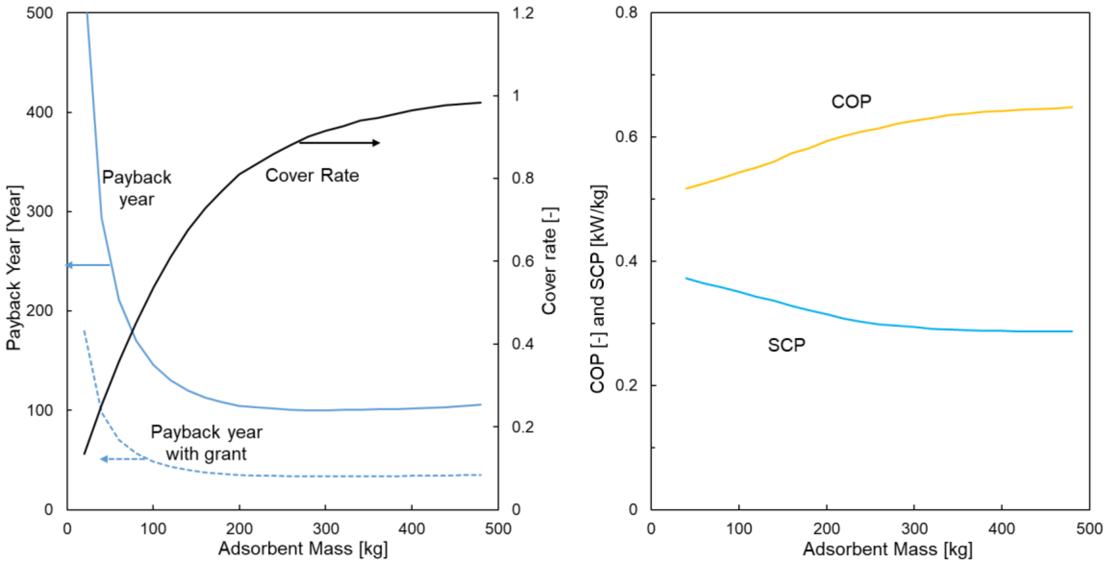

(a): Payback year and cover rate **(b): Annual average COP and SCP**

Fig. 6: Prediction results versus the adsorbent weight

adsorbent can't provide enough cooling capacity, at least 280 kg of adsorbent is necessary to improve CR and reduce payback year.

3.2.2. Hot water tank volume coefficient

The boiled hot water needs to be stored into the hot water tank. The larger hot water tank contributes to keep AC at a high regeneration temperature to provide high cooling performance. The volume of the hot water tank relative to the solar collector area, the Coe_{Vol} is changed from 20 L/m^2 to 200 L/m^2 at interval of 20 L/m^2. The $m_{\mathrm{adsorbent}}$ and the A_{SC} are fix as shown in **Tab.4**.

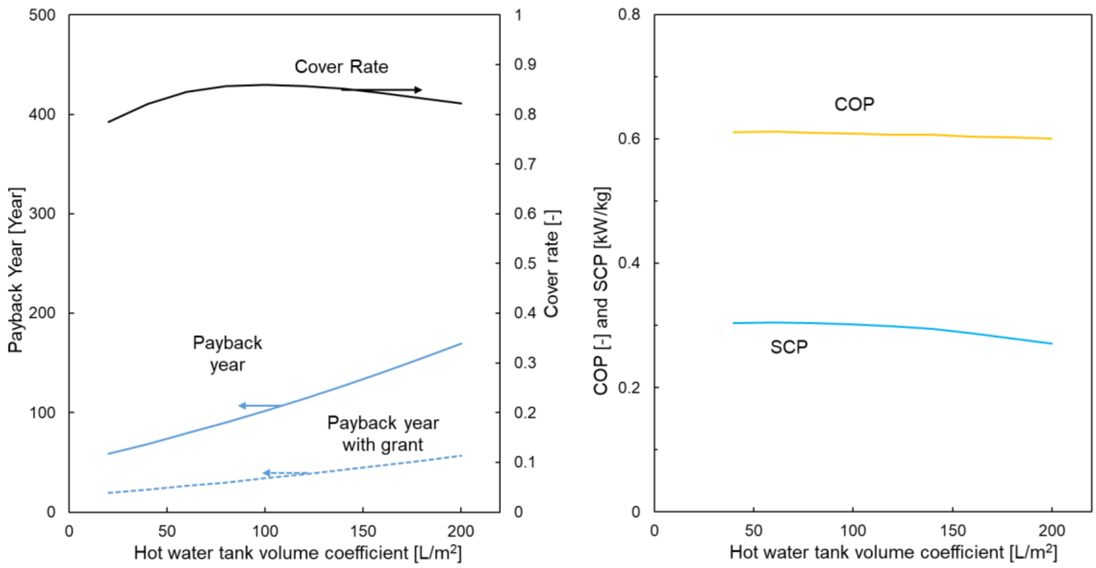

(a): Payback year and cover rate **(b): Annual average COP and SCP**

Fig. 7: Prediction results versus the adsorbent weight

As shown in **Fig.7(a)**. The *CR* is stable from 80 % - 85 % with slight fluctuation, it indicates that *CR* is unsensitive to the Coe_{Vol}. However, *PY* and PY_{grant} are increase with the increasing of the Coe_{Vol}. Obviously, small is a smart strategy to reduce the cost while a relatively high *CR* is kept. The highest *CR* of 85.89 % can be obtained while Coe_{Vol} of 100 L/m^2 is taken, meanwhile *PY* and PY_{grant} are 101.9 years and 34.0 years, respectively.

The annual average COP and SCP are shown in **Fig.7(b)**. Mildly decrease of both COP and SCP can be observed with the Coe_{Vol} grow larger than 100 L/m^2. The excess hot water tank volume results in larger heat loss that can't be covered by the solar collector. For the case that Coe_{Vol} is 100 L/m^2, COP and SCP are 0.61 and 0.3 kW/kg, respectively.

3.2.3. Solar collector area

Then the solar collector area A_{SC} is change from 50 m^2 to 2400 m^2 at interval of 50 m^2 while $m_{adsorbent}$ and the Coe_{Vol} is fix as shown in **Tab.4**. The prediction results are shown in **Fig.8**.

CR improve rapid and over 80 % while with the A_{SC} increase up to 850 m^2, then *CR* approaches 92 % slowly. The *PY* and PY_{grant} are reduced down to 68.0 years and 22.7 years respectively while the A_{SC} is 500 m^2. The insufficiency of the solar collector area leads to this result. Both *PY* and PY_{grant} start to rebound for the cases that A_{SC} is bigger 500 m^2. Thus, more than 500 m^2 is necessary in this study.

As shown in **Fig.8(b)**, the annual average SCP keep mildly increasing with the A_{SC} increasing. The larger A_{SC} contributes larger heat capacity for the regeneration heat to increase the annual average SCP, especially in cases that the heat load is extremely high to drop the temperature of the stored hot water. On the other hand, the annual average COP is almost constant around 0.6.

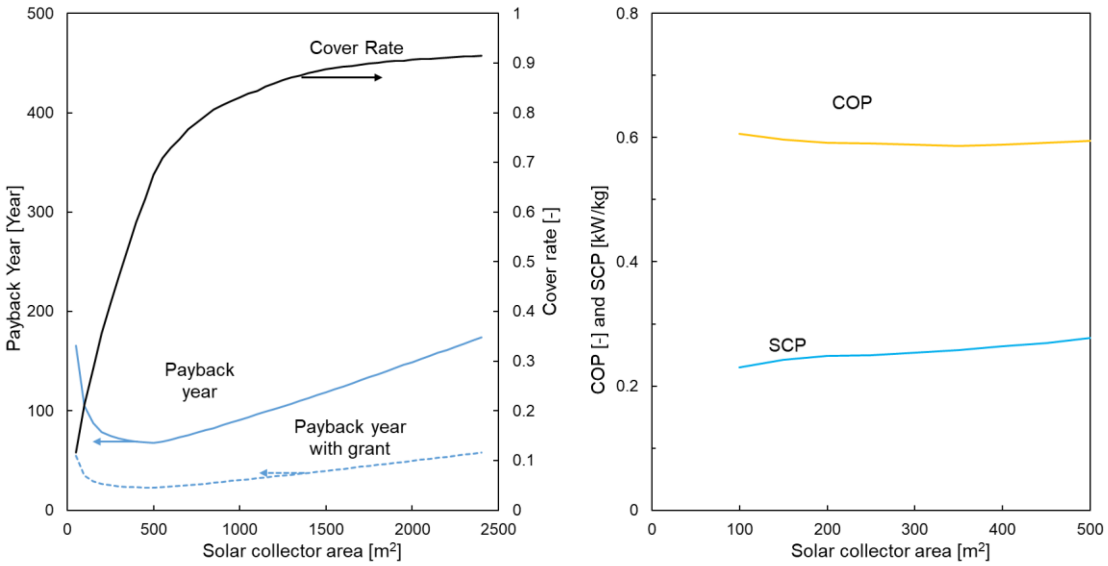

(a): Payback year and cover rate **(b): Annual average COP and SCP**

Fig. 8: Prediction results versus the adsorbent weight

3.4. System optimization

All the parameters of A_{SC}, $m_{adsorbent}$ and Coe_{Vol} are optimized in this section.

The ranges of the A_{SC}, $m_{adsorbent}$ and Coe_{Vol} are set as they're changed in the sections above to to obtain the shortest payback year with grant. In addition, the lowest *CRs* are limited as the extra conditions. The results are shown in **Tab.5**.

Without the limitation of *CR*, the smallest PY_{grant} of 7.6 years and *PY* of 54.1 years are achieved, relatively. It is an acceptable period for the commercial produce. Though *CR* of AC system is only 50.05 %, the AC system can be combined with other air-conditioner to provide sufficient cooling capacity for the factory and office building due to their large cooling capacity requirement. A_{SC} and $m_{adsorbent}$ are 250 m^2 300 kg respectively, it contributes compaction of the AC system. The 20 L/m^2 of Coe_{Vol} proved that the large hot water tank volume is not necessary.

On the other hand, only one domestic air-conditioner is introduced for every family, thus the lower limitation of *CR* is 80 %. While A_{SC}, $m_{adsorbent}$ and Coe_{Vol} are 600 m^2, 460 kg and 20 L/m^2 respectively, the *CR* of 80.39 % can be obtained. The PY_{grant} increased up to 9.6 years and the *PY* increase up to 58.5 years, which are still acceptable. Compared with the case that *CR* is 50.05 %, annual average COP is improved up to 0.64 from 0.61

Tab. 5: Optimization results

Coverate	**50.05 %**	**60.74 %**	**70.81 %**	**80.39 %**	**90.28 %**
$m_{\mathrm{adsorbent}}$ [kg]	300	380	360	460	460
Coe_{Vol} [L/m^2]	20	20	20	20	40
A_{SC} [m^2]	250	300	450	600	900
Annual average COP [-]	0.61	0.63	0.63	0.64	0.64
Annual average SCP [kW/kg]	0.28	0.28	0.29	0.29	0.29
Annual electricity consumption reduction [kWh]	10150.1	12318.9	14360.9	16304.8	18309.4
Annual CO_2 emmision reduction [ton]	4.415	5.359	6.247	7.093	7.965
PY	54.1	55.8	51.31	58.5	69.5
PY_{grant}	7.6	7.7	8.3	9.6	14.3

and SCP is improved up to 0.29 kW/kg from 0.28 kW/kg. The annual electricity consumption of 16304.8 kWh, which equivalent to 7.093 tons of CO_2 emission, can be reduced.

In order to improve CR up to 90.28 %, A_{SC} and Coe_{Vol} need to be increased to 900 m^2 and 40 L/m^2, respectively. It results in higher initial cost, the PY_{grant} increase up about 50 % to 14.3 years. However, the annual electricity consumption and its equivalent of the CO_2 emission only improved about 12.3 %, the improvement of the annual average COP and SCP are ignorable. This strategy can be applied to some large-scale and long-term projects with abundant financial support, such as the government building.

4. Conclusion

This study focuses on the annual cooling performance prediction of the (AC). A numerical model of AC system was established for the annual cooling performance prediction and parameter study. The following conclusion were obtained.

- The well-fit approximate functions of COP and SCP were built, they were applied for the rapid COP and SCP calculation.
- A numerical model of AC system was established for the annual cooling performance prediction and parameter study.
- Both A_{SC} and $m_{\mathrm{adsorbent}}$ can be determined to achieve the smallest PY_{grant}, however, the PY_{grant} is unsensitive to the Coe_{Vol}.
- PY_{grant} are 7.6 years, 7.7 years, 8.3 years, 9.6 years and 14.3 years while CR are 50.05 %, 60.07 %, 70.81 %, 80.39 % and 90.28 %, respectively.

5. References

Akahira A., Alam K.C.A., Hamamoto Y., Akisawa A., Kashiwagi T.. Mass recovery adsorption refrigeration cycle - improving cooling capacity. Refrigeration 2004;27:225–34.

He F., Nagano K., Togawa J.. Experimental study and development of a low-cost 1kW adsorption chiller using composite adsorbent based on natural mesoporous material. Energy 2020;209:118365.

He F., Nagano K, Seol S.H, Togawa J. Thermal performance improvement of AHPusing corrugated heat exchanger by dip-coating method with mass recovery.Energy 2022;239:122418.

He F., Nagano K., Togawa J.. Performance prediction of an adsorption chiller combined with heat recovery and mass recovery by a three-dimensional model. Energy 2023;277:127541.

J. Romero R., Rivera W., Gracia J., Best R.. Theoretical comparison of performance of an absorption heat pump system for cooling and heating operating with an aqueous ternary hydroxide and water/lithium bromide. Appl Therm Eng 2001;21:1137–47.

Jung-Yang San, Tsai Fu-Kang. Testing of a lab-scale four-bed adsorption heat pump. Appl Therm Eng 2014;70:274–81.

Lu Z.S., Wang R.Z.. Performance improvement by mass-heat recovery of an innovative adsorption air-conditioner driven by 50-80 ℃ hot water. Appl Therm. Eng 2013;55:113－20.

Liu H., Nagano K., Morita A., Togawa J., Nakamura M.. Experimental testing of a smallsorption air cooler using composite material made from natural siliceous shale andchloride. Appl Therm Eng 2015;82:68–81.

Manu S., Chandrashekar T.K.. A simulation study on performance evaluation of single-stage LiBr–H2O vapor absorption heat pump for chip cooling. Sustain Build Environ 2016;5:370–86.

Nakabayashi S., Nagano K., Nakamura M., Togawa J., Kurokawa A.. Improvement ofwater vapor adsorption ability of natural mesoporous material by impregnatingwith chloride salts for development of a new desiccant filter. Adsorption 2011;17:675–86.

Pan Q.W., Wang R.Z.. Experimental study on operating features of heat and massrecovery processes in adsorption refrigeration. Energy 2017;135:361–9.

Pan Q.W., Wang R.Z.. Study on operation strategy of a silica gel-water adsorption chiller in solar cooling application. Sol Energy 2018;172:24–31.

Srikhirin P., Ahpornratana S., Chungpaibulpatana S.. A review of absorption refrigeration technologies. Renew Sustain Energy Rev 2001;5:343–72.

Sapienza A., Santamaria S., Frazzica A., Freni A.. Influence of the management strategy and operating conditions on the performance of an adsorption chiller. Energy 2011;36:5532–8.

Seol S.H., Nagano K., Togawa J.. Modeling of adsorption heat pump system based onexperimental estimation of heat and mass transfer coefficients. Appl Therm Eng2020;171:115089.

Togawa J., Kurokawa A., Nagano K.. Water sorption property and cooling performance using natural mesoporous siliceous shale impregnated with LiCl for adsorption heat pump. Appl Therm Eng 2020;173:115241.

Appendix: Units and Symbols

Tab. 6: Nomenclature

Quantity	Symbol	Unit
Area	A	m^2
Constant coefficient	$\boldsymbol{a}_n$, $\boldsymbol{b}_n$, n =1,2,3,4,5	
Specific heat	c	kJ kg^{-1} K^{-1}
Irradiance	E	kW m^{-2}
Emission coefficient	*Emission*	kg kWh^{-1}
Specific enthalphy	*en*	kJ kg^{-1}
Heat loss coefficient	F_L	kW m^{-2} K^{-1}
Sensible heat	$H_{sensible}$	kJ kg^{-1}
Mass	m	kg
Mass flow rate	$\dot{m}$	kg s^{-1}
Price of CO_2 emmsion	$Price_{co2}$	JPY kWh^{-1}
Price of electricity	$Price_{ele}$	JPY kWh^{-1}
Heat	Q	kJ
Heat flow rate	$\dot{Q}$	W
Relative humidy	RH	
Temperature	T	K
Time	t,	s

Tab. 7: Greek Symbols

Quantity	Symbol	Unit
Density	ρ	kg m^{-3}
Efficiency	η	

Tab. 8: Subscripts

Quantity	Symbol
Regeneration	Reg
Sorption	Sor
Cycle Perido	cyc
Water	w
Solar collector	SC
Dry bulb	drybulb
Wet bulb	wetbulb
Cooling tower outlet	ct-out
Sorption adsorber outlet	sor-out
Adsorption chiller	ac
Initial cost	ini
Compress type air-conditioner	com
Electricity	ele
CO_2	co2
Volume	Vol
Hot water tank	HT
Maximum	Max
Spectral	λ